PLOS COMPLEX SYSTEMS

RESEARCH ARTICLE

Synergistic integration of fragmented transportation networks: When do networks (not) synergize?

Takahiro Ezaki[1]*, **Naoto Imura**[1], **Katsuhiro Nishinari**[1,2]

1 Research Center for Advanced Science and Technology, The University of Tokyo, 4-6-1 Komaba, Meguro-ku, Tokyo 153-8904, Japan, **2** Department of Aeronautics and Astronautics, School of Engineering, The University of Tokyo, 7-3-1 Hongo, Bunkyo-ku, Tokyo 113-8656, Japan

* tkezaki@g.ecc.u-tokyo.ac.jp

Citation: Ezaki T, Imura N, Nishinari K (2024) Synergistic integration of fragmented transportation networks: When do networks (not) synergize? PLOS Complex Syst 1(3): e0000017. https://doi.org/10.1371/journal.pcsy.0000017

Editor: Gaoxi Xiao, Nanyang Technological University, SINGAPORE

Received: May 4, 2024

Accepted: September 9, 2024

Published: November 5, 2024

Data Availability Statement: All the data and information to replicate the results are shown in the article.

Funding: This study was partially supported by Japan Society for the Promotion of Science (JSPS), Grants-in-Aid for Scientific Research (KAKENHI; Grant No. 24H02203 to TE). The funder had no role in study design, data collection and analysis, decision to publish, or preparation of the manuscript.

Competing interests: The authors have no competing interests to disclose.

Abstract

The transportation of information, goods, people, and other entities inevitably experiences fluctuations in demand and supply, which results in the underutilization of certain links within a transportation network while other links are fully utilized and unable to accommodate any additional demand. A promising strategy for leveraging these links is the collaborative integration of fragmented transportation networks to facilitate access between isolated nodes. We present a novel analytical framework for examining the conditions under which such network integration would enhance the overall transportation efficiency. We conducted comprehensive numerical experiments to investigate the influence of the network structure on the synergistic effects of network integration with a focus on the link survival ratio and dissimilarity between networks. The results showed that networks comprising nodes with relatively uniform importance benefit significantly from network integration whereas core–periphery networks are less likely to benefit. Based on our findings, we propose an indicator for predicting the potential for synergistic effects that is related to the growth rate of the giant component. This study contributes understanding of transportation network dynamics and offers practical insights for optimizing network integration strategies to leverage underutilized capacities and improve various types of transportation systems.

Author summary

We investigated the effects of integrating two transportation networks to leverage the excess transportation capacity left behind by fluctuations in demand or fragmented by disasters. We developed an analytical framework and conducted numerical experiments to identify conditions under which network integration is beneficial. Networks with uniformly important nodes benefit significantly while core–periphery networks benefit less. Based on our results, we propose an indicator for predicting the synergistic effect. This paper offers practical strategies for integrating transportation networks to improve

performance amid fluctuating demands and provides insights for stakeholders in logistics, supply chain, urban planning, and infrastructure developments.

Introduction

Transportation networks are systems that move information, goods, people, and other tangible or nontangible entities, which can be found in diverse sectors such as telecommunications, public transit, logistics, and power distribution. It is relatively rare for the capacity of transportation networks to be fully utilized due to fluctuations in demand and supply while most links are often fully utilized when the system operates under limited cost constraints [1–3]. In addition, temporary disruptions due to disasters or malfunctions [4–6] result in fragmented networks where the remaining capacity is underutilized.

One strategy for leveraging these fragmented networks is to integrate them with other fragmented networks, which facilitates access to isolated nodes, by opening up new paths to meet demand. In the context of logistics, the integration of multiple delivery networks or modes of delivery to improve cost efficiency and reduce CO_2 emissions is a topic of active discussion [7, 8]. Similarly, the arrangement of alternative transportation during service interruptions or periods of excessive demand in public transit systems [9, 10] and the adaptive assignment of passengers to flights within airline alliances [11, 12] can be considered forms of network integration. Thus, such an approach is gathering growing interest for the sustainable operation of various systems, but its theoretical foundations have not yet been fully established.

The efficient design and control of transportation networks have been extensively studied in various domains. For instance, theoretical research on complex networks has focused on maximizing the overall flow [13, 14], as well as optimizing redundancy [15, 16] and critical links [17–20] for enhanced robustness. Other studies have explored the impacts and mechanisms of integrating multiple transportation networks [21–25]. Morris and Barthelemy [26] found a nontrivial optimal coupling level of two networks to maximize their utility that depends on the source–sink distribution. Also, Li et al. [27] showed that assortative coupling decreases the transportation capacity of multilayer networks. From a more practical perspective, other studies have focused on the transportation dynamics of empirical systems such as urban transportation networks [28, 29] and airline multiplexity [11, 12]. Another related research field is percolation theory, which has been widely used to study the connectivity and fragmentation of networks [30–36]. In the context of transportation networks, it has been used to explain their dynamics [37–41]. Also, the percolation on multilayer networks has been studied from theoretical perspectives [33, 34].

Despite the substantial contributions of the above studies, they do not provide a satisfactory answer to the following question: What types of transportation networks demonstrate a synergistic effect from integration? There are several reasons for this. First, the above studies did not focus on the case where each layer of the integrated networks is fragmented (i.e., highly congested scenarios where most of the transportation capacity is already utilized), so they provide limited understanding of the mechanisms that give rise to synergistic effects, such as the recovery of disconnected paths. Second, they mostly focused on a specific network structure or small number of network structures such as Erdős–Rényi, Barabási–Albert (BA), and empirical networks [25], so they do not clarify which types of network structures lead to a synergistic effect when integrated. Finally, percolation theory can be used to roughly estimate the critical link density for emergence of the giant component, but its contributions to transportation dynamics are not straightforward.

In this study, we developed a novel analytical framework and conducted extensive numerical experiments to explore the synergistic effects of integrating two fragmented networks. Our contributions are two-fold. First, we focused on integrating fragmented networks with similar network structures because this scenario is expected to yield the least synergistic effects, which allowed us to develop an indicator for estimating the magnitude of the synergistic effect that is related to the growth of the giant component. Then, we confirmed that integrating networks with different structures yields substantial synergistic effects.

Results

Integration of networks with similar structures

As shown in Fig 1, we generated two fragmented networks from a single network by randomly preserving the same fraction of links (i.e., link survival ratio, denoted by r), while ensuring that a specified fraction of non-overlapping links (i.e., dissimilarity, denoted by d) was controlled. We then overlaid these networks and randomly selected one node in each as the source and sink while avoiding overlapping. This allowed us to simulate the integration of two fragmented networks with the same underlying network structure. We then computed the maximum flow [42, 43] between the source and sink nodes through the links of the integrated network, which we used as a measure of the transportation capability [44–46].

Fig 2A shows the maximum flows of the integrated networks with different link survival ratios and dissimilarities. The integrated network with $d = 0$ (i.e., two fragmented networks were identical) demonstrated no synergistic effect (i.e., the maximum flow of the integrated network was equal to the sum of the maximum flows of the two fragmented networks), and the average maximum flow of the integrated network coincided with the sum of the maximum flows calculated separately for the two fragmented networks for any values of d. Therefore, we evaluated the presence of a synergistic effects by comparing the results of the integrated networks with those obtained under the condition $d = 0$. For a majority of network structures considered in this study (i.e., grid, random, BA, and power), a substantial synergistic effect was observed where the maximum flow increased with increasing d. In some cases, the synergistic effect was substantial even when d was not excessively large (e.g., $d = 0.5$). Conversely, for the

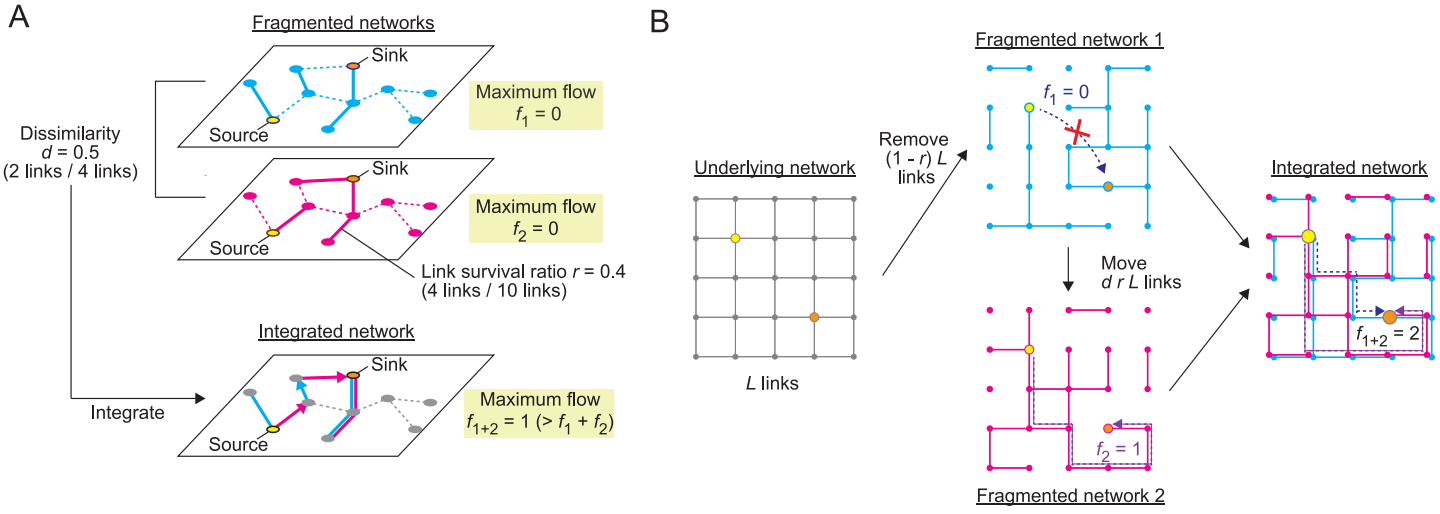

Fig 1. Integration of fragmented transportation networks with similar structures to evaluate the synergistic effect. (A) Schematic of the experimental procedure. (B) Example of the integration of two fragmented networks generated from a grid network.

https://doi.org/10.1371/journal.pcsy.0000017.g001

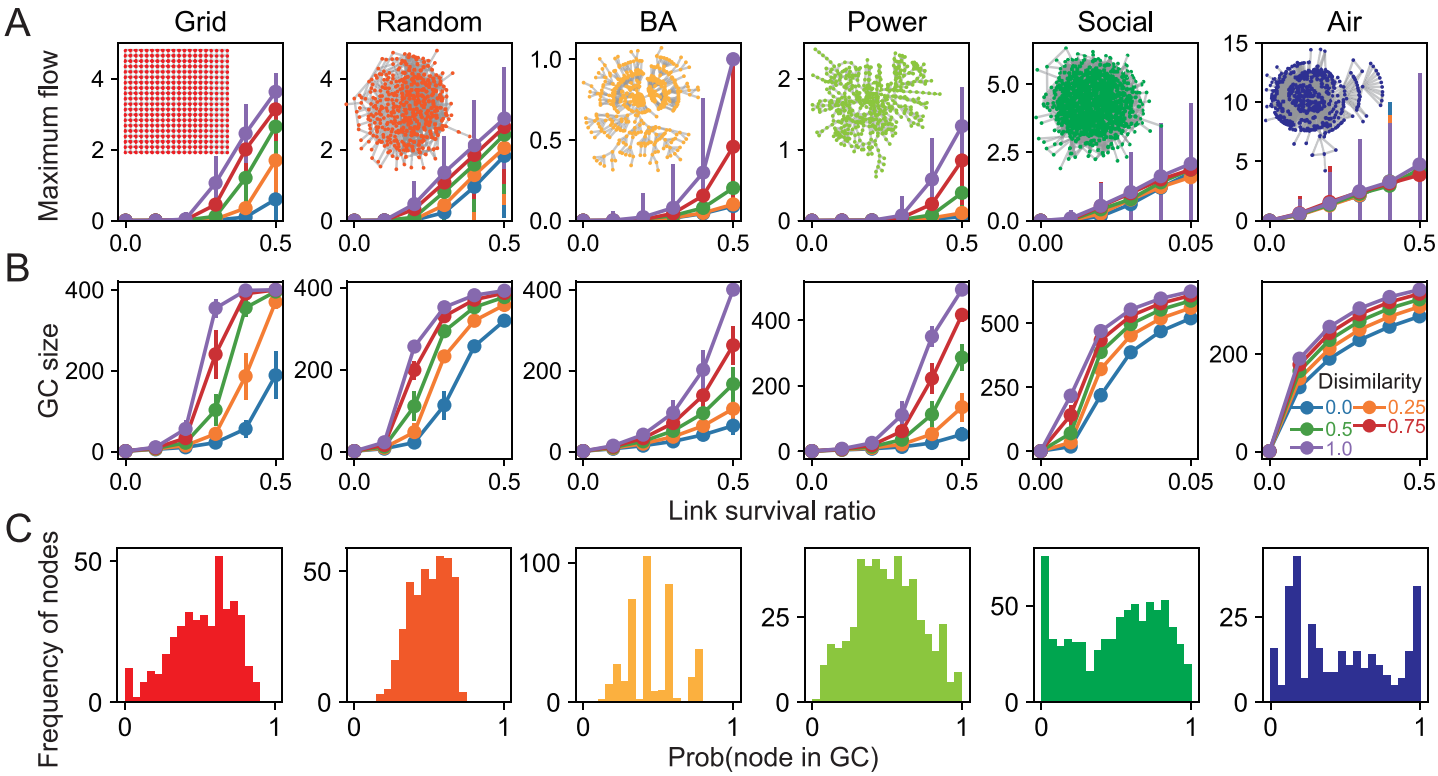

Fig 2. Synergistic effect in different network types: (A) Maximum flow as a function of the link survival ratio r and dissimilarity d. (B) Size of the giant component. We evaluated $0 \leq r \leq 0.05$ for the social network because it had a much greater link density than the other networks. (C) Propensity of each node to be included in the giant component under controlled conditions. The error bars in the graphs represent the standard deviation computed based on 1000 samples.

https://doi.org/10.1371/journal.pcsy.0000017.g002

social and air transportation network, the maximum flow exhibited only a minor dependence on d.

We investigated whether this behavior could be explained by the size of the giant component (i.e., the number of nodes in the largest connected component) of the integrated networks. In general, the majority of nodes became connected once the link survival ratio r exceeded a threshold value. Because nonzero flow can occur within the same connected component, the behavior of the giant component seems a likely indicator of the utility of the integrated network. However, Fig 2B shows that the growth pattern of the giant component was not directly reflected by an increase in the maximum flow. More importantly, for networks with no synergistic effect, the size of the giant component increased with increasing d. In other words, the size of the giant component of the integrated network could not simply explain the synergistic effect on its own. We also confirmed that the small-worldness and link density of the network did not significantly influence the synergy (see Fig A1 in S1 Appendix).

Next, we analyzed the propensity of each node to be included in the giant component. Fig 2C shows the distributions of the propensity of each node to be included in the giant component under controlled conditions (see Materials and methods for details). Note that nodes with a higher propensity are more likely to be part of the giant component, indicating their centrality within the network, while those with a lower propensity are typically situated on the periphery. Networks that exhibited a synergistic effect generally had a unimodal distribution of nodes. In contrast, the social and air transportation networks demonstrated a bimodal distribution of core nodes with a high propensity and peripheral nodes with a low propensity. We

also performed k-shell decomposition analysis [47, 48] and found that the social and air transportation networks had prominent core–periphery structure (see Fig A2 in S1 Appendix). Thus, we hypothesized that a core–periphery network structure could be a key factor that determines the absence of a synergistic effect.

Integration of core–periphery networks

To validate the above hypothesis, we employed a generative model to allow for continuous interpolation between random networks and core–periphery networks (by a parameter γ) and between hub–spoke and layered types of core–periphery networks (by a parameter δ; see also Materials and methods) [49], and investigated the maximum flow of the integrated networks. Fig 3A and Fig A1 in S1 Appendix show that increasing the degree of the core–periphery structure (γ), diminished the synergistic effect. We can also confirm that the size of the giant component depended on d (Fig 3B) even when the distribution of the propensity of each node to be included in the giant component was strongly separated, where the larger peak consisted of core nodes (Fig 3C). To gain a deeper understanding of this mechanism, we analyzed fragmented core–periphery networks (i.e., before integration) with strong separation between core and peripheral nodes ($\gamma = 10$). Fig 3D and 3E show the results, which we classified based on

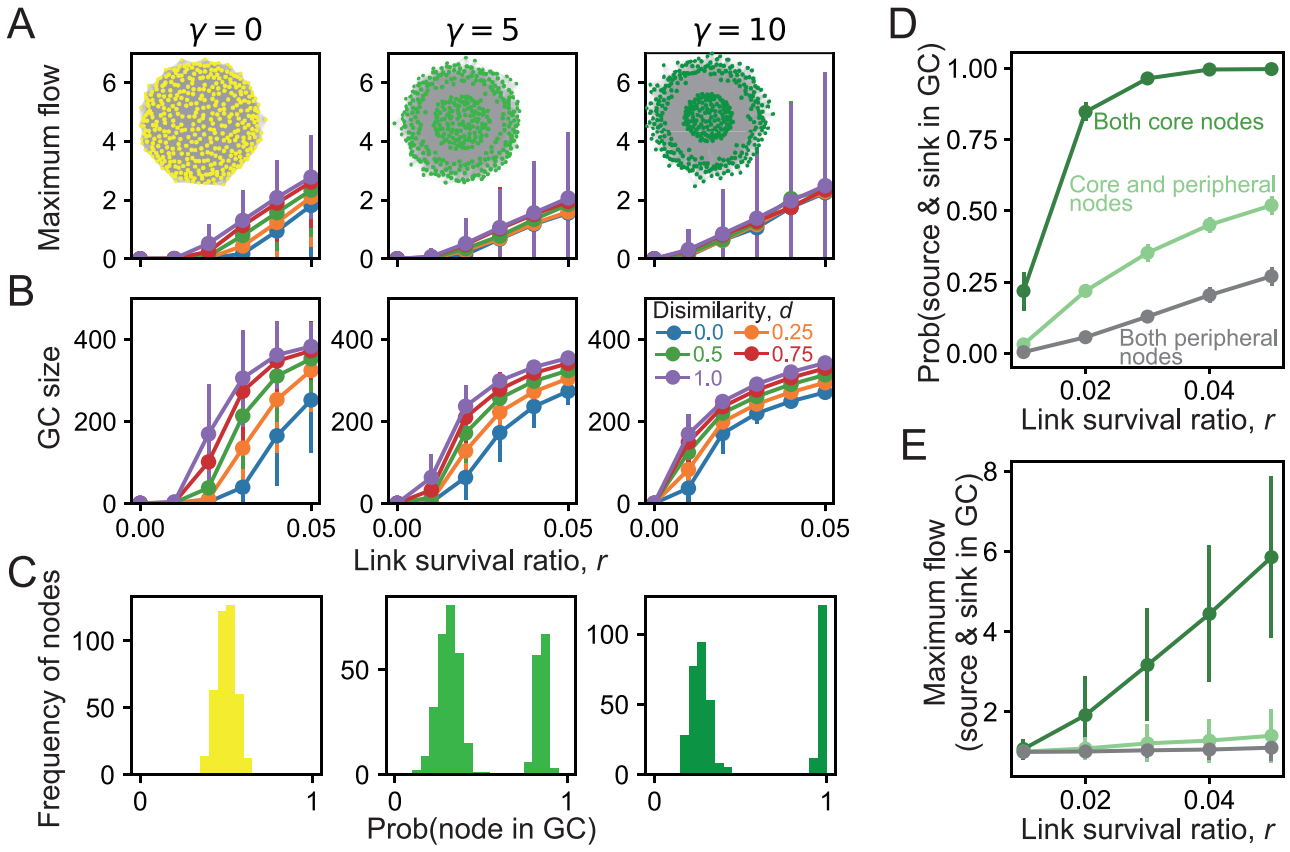

Fig 3. Synergistic effect in integrated networks according to the degree of the core–periphery structure (γ): (A) Maximum flow, (B) size of giant component, and (C) distribution of the propensity of each node to be included in the giant component. We set $\delta = 0$ (see Fig A3 in S1 Appendix for the results for $\delta = 1$). Network statistics for fragmented networks ($\delta = 0$, $\gamma = 10$): (D) probability of the source and sink nodes being included in the giant component and (E) maximum flow depending on whether the source and sink nodes are core and/or peripheral nodes. The error bars represent the standard deviation computed based on 1000 samples.

https://doi.org/10.1371/journal.pcsy.0000017.g003

whether the source and sink nodes were assigned to core nodes (which were predefined in the model). When both the source and sink nodes were assigned to core nodes, they were highly likely to be included in the giant component (i.e., a nonzero maximum flow existed) even at low r. Moreover, the resulting maximum flow was substantially larger than that obtained when at least one of the source or sink nodes was assigned to a peripheral node.

In other words, the expected maximum flow was determined by the maximum flow between nodes within the core, and these nodes had a high probability of being connected even at low r. The newly accessible nodes from network integration, which was the origin of the synergistic effect, were mostly on the periphery. Consequently, the additional transportation capacity gained from these nodes was relatively small.

Consistent with this observation, we found that the synergistic effect was decreased when we increased the number of core nodes (see Fig A1 in S1 Appendix).

Predicting the magnitude of the synergistic effect

Next, we attempted to predict the magnitude of the synergistic effects based on the network structure. For core–periphery networks, the core nodes became connected abruptly at a relatively low r while the peripheral nodes gradually became connected with increasing r (Fig 3D). Conversely, for homogeneous networks, the majority of nodes became connected abruptly when r reached a certain threshold (Fig 2B). In the latter case, the increase in links due to network integration should result in a larger synergistic effect because it enables access to many new nodes. Therefore, we developed an indicator of the synergistic effect obtained through network integration by quantifying the "cost" (i.e., additional link survival ratio required) to increase the size of the giant component. Fig 4 shows the cost normalized by the link survival ratio for a giant component size of half the network (see Materials and methods for details).

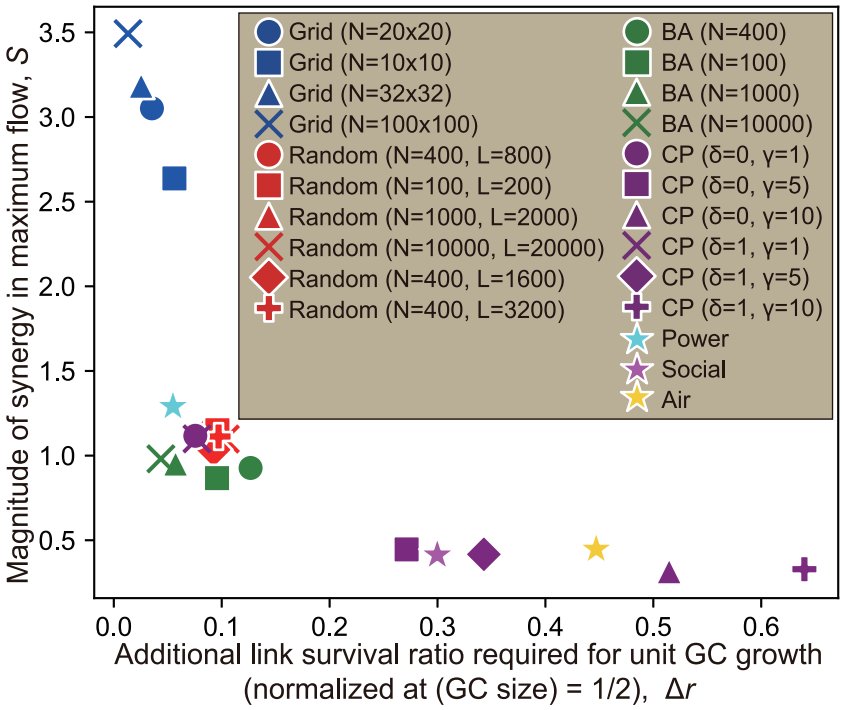

Fig 4. Magnitude of the synergistic effect of network integration vs the cost of increasing the giant component for different network structures with different numbers of nodes (N) and links (L).

https://doi.org/10.1371/journal.pcsy.0000017.g004

Despite its simplicity, the indicator well explained the potential synergistic effect of a vast majority of networks tested, which included not only different network structures but also different numbers of nodes and link densities.

Integration of networks with different structures

The previous results were focused on the effects of integrating networks with the same underlying structure. Here, we report the results concerning the integration of fragmented networks with different underlying network structures.

First, we compared the sum of the maximum flows of the individual fragmented networks before integration, against the maximum flow of the integrated network. We integrated different pairs of the networks in Fig 2, where the labels of the nodes for integration were randomly assigned. When the networks with different numbers of nodes were integrated, the larger network had nodes that did not correspond to any nodes in the smaller network. The source and sink nodes were selected from the nodes common to both networks. Because different network structures were being integrated, the dissimilarity d could not be defined in a manner consistent with that used in the previous experiments. Fig 5 shows that network integration resulted in a substantial increase in the maximum flow for all cases. The synergistic effect was particularly prominent in cases involving the grid or power networks.

Finally, we investigated the effects of integrating networks with different core–periphery structures. Networks with the same number of nodes were integrated without randomization to control the position of core nodes. We considered three cases: two networks with the same core–periphery structure, a core–periphery network and random network, and two core–periphery networks with different (i.e., non-overlapping) core nodes. Fig 6 shows that network integration had a substantial synergistic effect in terms of the maximum flow. However, the dominance of the core–periphery network limited the extent of the synergistic effect when integrated with random network structures. These results indicate that a core–periphery network may need to be integrated with another network having a complementary core–periphery structure to achieve the desired synergistic effect.

Discussions and conclusions

We developed an analytical framework for evaluating the synergistic effect of integrating fragmented transportation networks and obtained the following conclusions: (i) Substantial synergistic effect was observed from integrating a wide range of network structures but not in networks with the same core–periphery structure. (ii) The magnitude of the synergistic effect could be explained to some extent by observing the growth rate of the giant component. (iii) A synergistic effect was observed when fragmented networks with different core–periphery structures were integrated.

Our results have various theoretical and practical implications. From a theoretical perspective, the established relationship between the cost of the additional link survival ratio to increase the giant component and the expected magnitude of the synergistic effect (Fig 4) may suggest an important logical link between percolation theory and the maximum flow problem. Because the integration of two networks effectively increases the number of links and thus increases the size of the giant component, it is not surprising that there is some relationship between them. However, the fact that the maximum synergistic effect which is achieved for various link survival ratios is well explained only by the feature of the giant component in the vicinity of $r = r_{0.5}$ is nontrivial. We selected the link survival ratio when the giant component was half the size of the total network ($r_{0.5}$) as the standard value because of the naive intuition that this point typically represents the percolation behavior in most networks. However,

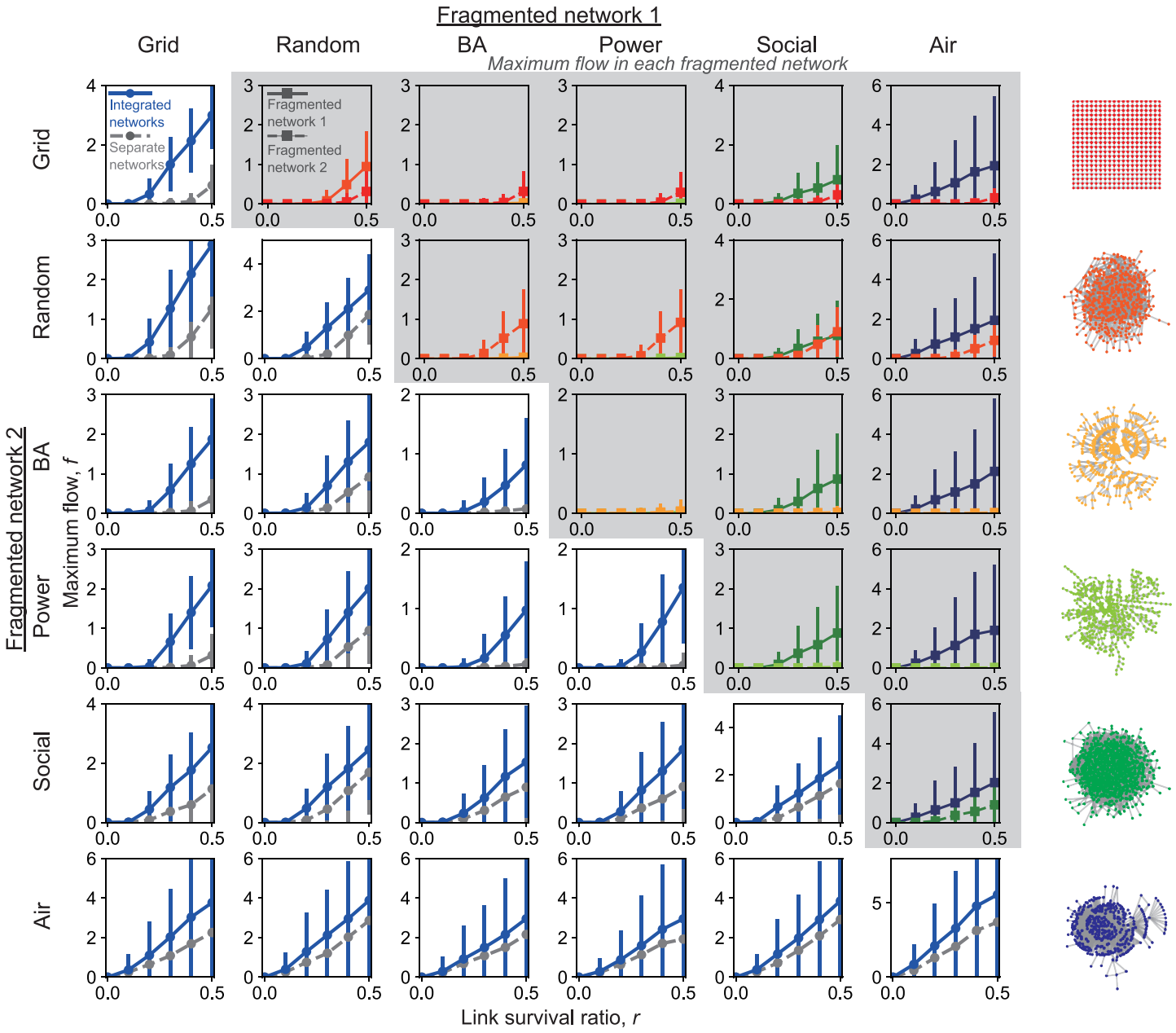

Fig 5. Synergistic effect of integrating networks with different structures. Two fragmented networks were integrated with the same link survival ratio r except for the social network. In this case, $r/10$ was used given its particularly high link density. The shaded area shows the separate maximum flow for each fragmented network. The error bars represent the standard deviation computed based on 1000 samples.

https://doi.org/10.1371/journal.pcsy.0000017.g005

developing a rigorous theoretical interpretation of this observation as well as more refined metrics remains an open challenge.

From a practical perspective, many airline networks [50, 51] and logistics networks [52, 53] have a core–periphery structure. For such networks, collaboration between different transportation modes (e.g., air and sea) rather than within the same transportation mode can potentially lead to a larger synergistic effect. Additionally, for spatial networks such as road networks and power grids that are less likely to have a strong core–periphery structure, a

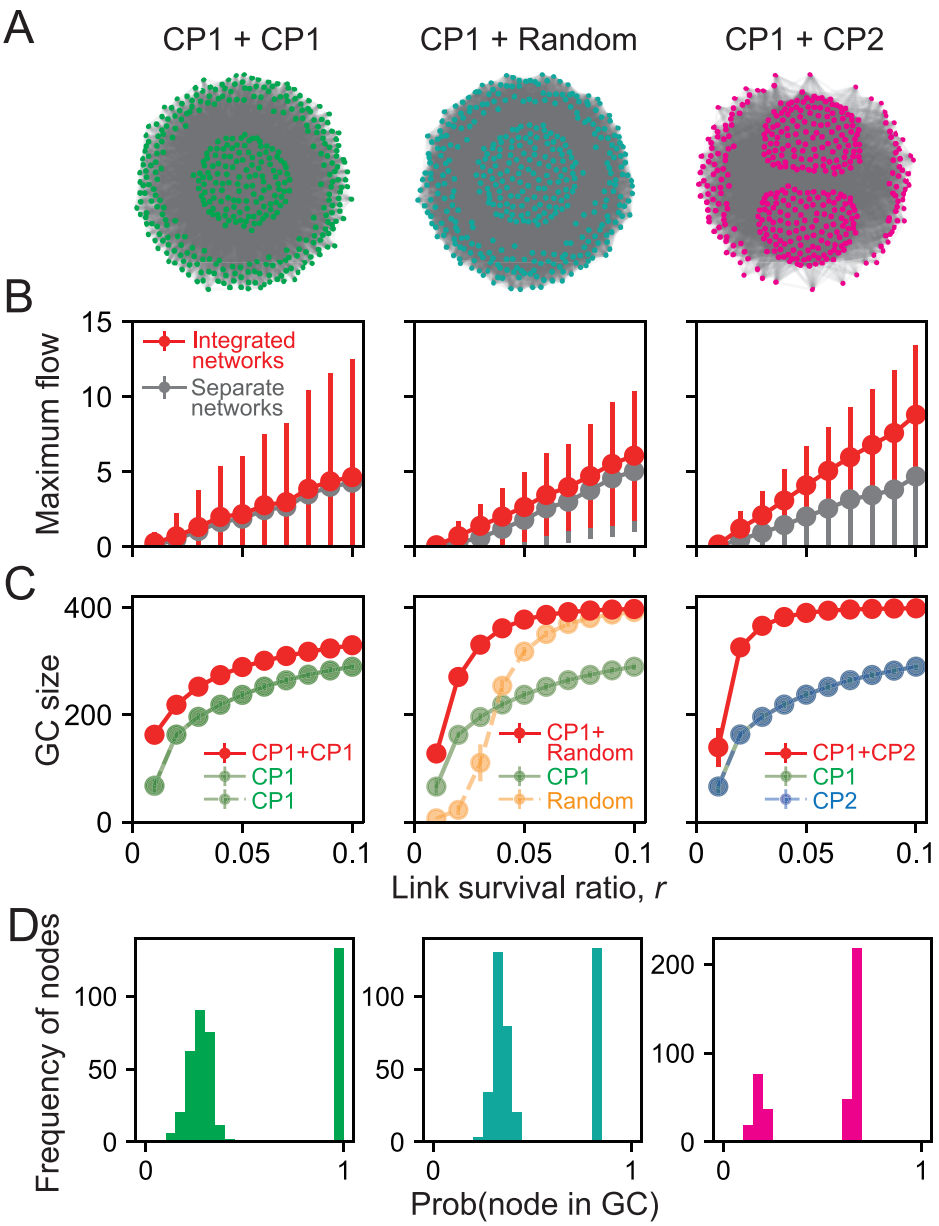

Fig 6. Synergistic effect of integrating networks with different core–periphery structures. (A) Types of integrated networks. CP1 and CP2 were core–periphery networks with different core nodes ($\delta = 0$, $\gamma = 10$). The random network was generated by setting $\delta = 0$ and $\gamma = 0$. (B) Maximum flow in the integrated networks. (C) Giant component size in the integrated networks. (D) Distribution of the propensity of each node to be in the giant component. The error bars represent the standard deviation computed based on 1000 samples.

https://doi.org/10.1371/journal.pcsy.0000017.g006

synergistic effect can generally be expected with network integration. However, it is important to note that the specific applicability of these findings may vary depending on the particular constraints and objectives of infrastructural optimization.

In this study, we considered a uniform random and independent fragmentation process across two networks. However, these conditions may not consistently apply in real-world situations. First, traffic demands are often not randomly distributed [54, 55]. Second, the availability of each link is determined by the relationship between supply and demand, which leads to a

trade-off with costs that varies according to the situation [56, 57]. Third, networks with the same transportation mode may experience correlated demand, and the same links may be destroyed in cases of fragmentation due to disasters or damage. Even in such cases, the benefits of integrating networks with different structures are likely to remain valid. Incorporating these factors using real-world data [58, 59] is a very important topic for future research. For such an analysis, more detailed considerations would be required, such as the conditions for overlapping nodes (e.g., stations or stops) across different modes, the development of methods to quantify the differences between network pairs of varying sizes, and criteria for realistic link failures.

We used the expected maximum flow between two nodes to measure the performance of transportation networks. Because of the linearity of the maximum flow problem [43], similar conclusions can be expected even when multiple sources and sinks are considered [60], although congestion is likely to have marginal effects. Additionally, if various capacity values are assigned to each link and/or realistic origin–destination demands are considered, then the problem may become more complex and may exceed the scope of intuitive understanding. However, we can make some conjectures based on the findings of this study. If networks with different demands are integrated, the synergistic effect could be greater than that reported here because of the benefits of gaining access to new nodes and utilizing links that were previously unused in each network. In this case, the information gained in this study would still be useful. Also, in real-world networks, large transportation capacities are often allocated to critical links. In such cases, integrating networks with similar capacity distributions may yield a greater synergistic effect in leveraging high-capacity links than integrating networks with dissimilar capacity distributions. For example, integrating core–periphery networks with different cores may cause the links connecting the core to the periphery to become bottlenecks and prevent the full utilization of the higher capacity links. Thus, topological and capacity characteristics of the networks being integrated need to be considered. For such analysis, k-shell decomposition [47, 48] would be useful to evaluate the size of effective cores in the integrated network.

This study establishes a theoretical foundation for the integration of fragmented transportation networks. Our findings have a wide range of potential applications, spanning fields such as logistics, electric and water infrastructure, information and telecommunication networks, and public transit systems. Exploring these systems using real-world data will be a fascinating future endeavor.

Materials and methods

Integration of networks with the same network structure

We investigated the change in transportation capacity due to network integration as follows (Fig 1B). We generated two fragmented networks by using the following procedure: (i) We prepared the network for analysis. (ii) We randomly preserved the number of links specified by the link survival ratio ($0 \leq r \leq 0.5$) and removed the remaining links to generate network 1. (iii) We randomly replaced a fraction of links with links removed in (ii) as specified by the dissimilarity ($0 \leq d \leq 1$) to generate network 2. In this way, networks 1 and 2 had the same r but a fraction d of links in different positions.

We created an integrated network by superimposing the links of the two fragmented networks. If links were present at the same location, the transportation capacity was doubled. We measured the transportation capacity of network 1, network 2, and the integrated network by randomly selecting one source node and one sink node (commonly used in the three networks) and solving the maximum flow problem for each network. The maximum flow

represents the maximum amount of flow that can be sent from the source to the sink through links in the network, which we calculated by using the `maximum_flow()` function provided by the Python NetworkX library [61]. This function is based on the Ford-Fulkerson method [42, 43] and computes the maximum flow as follows: It iteratively searches for augmenting paths from the source to the sink in the residual graph, where each path represents a route along which additional flow can be sent. The algorithm increases the flow along these paths by the minimum capacity available on the path and updates the residual capacities accordingly. This process repeats until no more augmenting paths can be found, at which point the current flow represents the maximum flow in the network.

Unless otherwise stated, we performed 1000 experimental runs for each condition (i.e., choice of network, link survival ratio r, and dissimilarity d), where each run involved generating the networks, selecting the sink and source nodes, and computing the maximum flow. We recorded the average and standard deviation of the maximum flow for each condition.

Analyzed networks

We used the following undirected networks for the experiments, where the numbers of nodes and links were denoted by N and L, respectively. The results in Figs 2 and 5 were obtained under the conditions referred to as example cases. Each link was defined as having a transportation capacity of 1.

Grid network. The grid network was a square lattice with closed boundaries and a size of $l \times l$. In addition to the example case of $l = 20$ ($N = 400$), we also considered the cases of $l = 10$, 32, 100.

Random network. The random networks were generated by randomly selecting L links without duplication from the list of $N(N-1)/2$ possible pairs of nodes. In addition to the example case of $N = 400$, $L = 800$, we considered cases with $N = 100$, 1000, 10000 and $L = 1600$, 3200.

Barabási-Albert network. We used the Barabási-Albert network as representative of a network with scale-free properties [62]. The number of links m to be added when a new node is introduced was set to 1. In addition to the example case of $N = 400$, we also considered the cases of $N = 100$, 1000, 10000. The BA network was generated by using the `barabasi_albert_graph()` function provided by the Python NetworkX library [61].

Empirical networks. We considered three different empirical networks: a power grid, social network, and air transportation network [63]. The power grid had a size of $N = 494$, $L = 586$; the social network had a size of $N = 769$, $L = 1.7 \times 10^4$; and the air transportation network had a size of $N = 332$, $L = 2.1 \times 10^3$.

Core–periphery network. We created core–periphery networks by using the generative model proposed by Gallagher *et al.* [49]. The network was generated by a stochastic block model [64, 65] with a block matrix:

$$\begin{pmatrix} p\gamma & p & p(1-\delta)+\frac{p}{\gamma}\delta \\ p & p\delta+\frac{p}{\gamma}(1-\delta) & \frac{p}{\gamma} \\ p(1-\delta)+\frac{p}{\gamma}\delta & \frac{p}{\gamma} & \frac{p}{\gamma} \end{pmatrix}$$

Here, hub–spoke and layered types of core–periphery networks can be interpolated by using the parameter δ, and core–periphery and random networks can be interpolated by using the parameter γ. We generated networks under the conditions of $\delta = 0$ (purely hub–spoke type), $\delta = 1$ (purely layered type), and $\gamma = 1$ (purely random), $\gamma = 5$ (moderate link concentration to the core), and $\gamma = 10$ (strong link concentration to the core). We considered a network with

$N = 399$ nodes where 133 nodes were designated as core nodes, and the link generation probability p between nodes was fixed at $p = 0.01$.

Finding the link survival ratio for a given giant component size

For a single network under analysis, we used a bisection algorithm to find the link survival ratios at which the giant component becomes 0.5 and 0.6 times the total size of the network, which we denoted as $r_{0.5}$ and $r_{0.6}$, respectively. The expected value of the giant component size was calculated based on 10^4 fragmented networks generated randomly for each link survival ratio. The algorithm was iterated until the giant component size was within 0.2% of the target value.

Propensity of each node to be included in the giant component

For each network condition, we sampled a single network and found the value of $r_{0.5}$. Then, with the obtained link survival ratio, we randomly generated 1000 fragmented networks and counted how many times each node was included in the giant component. The obtained distributions are shown in Fig 2C.

Quantifying the synergistic effect and the characteristic growth rate of the giant component

The synergistic effect obtained by network integration was calculated as the maximum difference in the maximum flow f between the cases of dissimilarity $d = 0$ and 1 over various link survival ratios:

$$S = \max_r \{f(d = 1) - f(d = 0)\}.$$

We used the cost of increasing the giant component size as an indicator:

$$\Delta\bar{r} = \frac{r_{0.6} - r_{0.5}}{r_{0.5}}.$$

The indicator quantifies the magnitude of the additional link survival ratio required to increase the giant component from 0.5 to 0.6 times the total size of the network. The difference was divided by $r_{0.5}$ to standardize the link density in the network.

This analysis was performed by generating a single network of each type and calculating S and $\Delta\bar{r}$.

Supporting information

S1 Appendix. Supporting information for synergistic integration of fragmented transportation networks: When do networks (not) synergize? Results for additional experiments. (PDF)

Author Contributions

Conceptualization: Takahiro Ezaki.

Formal analysis: Takahiro Ezaki.

Investigation: Takahiro Ezaki.

Methodology: Takahiro Ezaki.

Project administration: Takahiro Ezaki, Naoto Imura, Katsuhiro Nishinari.

Supervision: Naoto Imura, Katsuhiro Nishinari.

Visualization: Takahiro Ezaki.

Writing – original draft: Takahiro Ezaki.

Writing – review & editing: Takahiro Ezaki, Naoto Imura, Katsuhiro Nishinari.

References

1. Marseguerra M, Zio E, Podofillini L, Coit DW. Optimal design of reliable network systems in presence of uncertainty. IEEE Transactions on Reliability. 2005; 54(2):243–253. https://doi.org/10.1109/TR.2005.847279
2. Ukkusuri SV, Mathew TV, Waller ST. Robust transportation network design under demand uncertainty. Computer-aided Civil and Infrastructure Engineering. 2007; 22(1):6–18. https://doi.org/10.1111/j.1467-8667.2006.00465.x
3. Chen A, Zhou Z, Chootinan P, Ryu S, Yang C, Wong SC. Transport Network Design Problem under Uncertainty: A Review and New Developments. Transport Reviews. 2011; 31(6):743–768. https://doi.org/10.1080/01441647.2011.589539
4. Faturechi R, Miller-Hooks E. Travel time resilience of roadway networks under disaster. Transportation Research Part B: Methodological. 2014; 70:47–64. https://doi.org/10.1016/j.trb.2014.08.007
5. Kim Y, Chen YS, Linderman K. Supply network disruption and resilience: A network structural perspective. Journal of Operations Management. 2015; 33-34:43–59. https://doi.org/10.1016/j.jom.2014.10.006
6. Çelik M. Network restoration and recovery in humanitarian operations: Framework, literature review, and research directions. Surveys in Operations Research and Management Science. 2016; 21(2):47–61. https://doi.org/10.1016/j.sorms.2016.12.001
7. Cruijssen F, Dullaert W, Fleuren H. Horizontal Cooperation in Transport and Logistics: A Literature Review. Transportation Journal. 2007; 46(3):22–39. https://doi.org/10.2307/20713677
8. Pan S, Trentesaux D, Ballot E, Huang GQ. Horizontal collaborative transport: survey of solutions and practical implementation issues. International Journal of Production Research. 2019; 57(15-16):5340–5361. https://doi.org/10.1080/00207543.2019.1574040
9. Du M, Zhou J, Chen A, Tan H. Modeling the capacity of multimodal and intermodal urban transportation networks that incorporate emerging travel modes. Transportation Research Part E: Logistics and Transportation Review. 2022; 168:102937. https://doi.org/10.1016/j.tre.2022.102937
10. Fan Y, Ding J, Liu H, Wang Y, Long J. Large-scale multimodal transportation network models and algorithms-Part I: The combined mode split and traffic assignment problem. Transportation Research Part E: Logistics and Transportation Review. 2022; 164:102832. https://doi.org/10.1016/j.tre.2022.102832
11. Cardillo A, Gómez-Gardeñes J, Zanin M, Romance M, Papo D, del Pozo F, et al. Emergence of network features from multiplexity. Scientific Reports. 2013; 3:1344. https://doi.org/10.1038/srep01344 PMID: 23446838
12. Du WB, Zhou XL, Lordan O, Wang Z, Zhao C, Zhu YB. Analysis of the Chinese Airline Network as multi-layer networks. Transportation Research Part E: Logistics and Transportation Review. 2016; 89:108–116. https://doi.org/10.1016/j.tre.2016.03.009
13. Danila B, Yu Y, Marsh JA, Bassler KE. Optimal transport on complex networks. Physical Review E. 2006; 74(4 Pt 2):046106. https://doi.org/10.1103/PhysRevE.74.046106 PMID: 17155132
14. Li G, Reis SDS, Moreira AA, Havlin S, Stanley HE, Andrade JS Jr. Towards design principles for optimal transport networks. Physical Review Letters. 2010; 104(1):018701. https://doi.org/10.1103/PhysRevLett.104.018701 PMID: 20366398
15. Corson F. Fluctuations and redundancy in optimal transport networks. Physical Review Letters. 2010; 104(4):048703. https://doi.org/10.1103/PhysRevLett.104.048703 PMID: 20366745
16. Ezaki T, Imura N, Nishinari K. Towards understanding network topology and robustness of logistics systems. Communications in Transportation Research. 2022; 2:100064. https://doi.org/10.1016/j.commtr.2022.100064
17. Rodríguez-Núñez E, García-Palomares JC. Measuring the vulnerability of public transport networks. Journal of Transport Geography. 2014; 35:50–63. https://doi.org/10.1016/j.jtrangeo.2014.01.008
18. Zhou Y, Wang J. Critical Link Analysis for Urban Transportation Systems. IEEE Transactions on Intelligent Transportation Systems. 2018; 19(2):402–415. https://doi.org/10.1109/TITS.2017.2700080

19. Woldeyohannes YT, Jiang Y. Measures for Network Structural Dependency Analysis. IEEE Communications Letters. 2018; 22(10):2052–2055. https://doi.org/10.1109/LCOMM.2018.2864109

20. Ezaki T, Imura N, Nishinari K. Reinforcing critical links for robust network logistics: A centrality measure for substitutability. Journal of Physics Communications. 2023; 7(2):025001. https://doi.org/10.1088/2399-6528/acb7c9

21. Mucha PJ, Richardson T, Macon K, Porter MA, Onnela JP. Community structure in time-dependent, multiscale, and multiplex networks. Science. 2010; 328(5980):876–878. https://doi.org/10.1126/science.1184819 PMID: 20466926

22. De Domenico M, Solé-Ribalta A, Cozzo E, Kivelä M, Moreno Y, Porter MA, et al. Mathematical Formulation of Multilayer Networks. Physical Review X. 2013; 3(4):041022. https://doi.org/10.1103/PhysRevX.3.041022

23. Boccaletti S, Bianconi G, Criado R, Del Genio CI, Gómez-Gardeñes J, Romance M, et al. The structure and dynamics of multilayer networks. Physics Reports. 2014; 544(1):1–122. https://doi.org/10.1016/j.physrep.2014.07.001 PMID: 32834429

24. Kivelä M, Arenas A, Barthelemy M, Gleeson JP, Moreno Y, Porter MA. Multilayer networks. Journal of Complex Networks. 2014; 2(3):203–271. https://doi.org/10.1093/comnet/cnu016

25. Wu J, Pu C, Li L, Cao G. Traffic dynamics on multilayer networks. Digital Communications and Networks. 2020; 6(1):58–63. https://doi.org/10.1016/j.dcan.2018.10.011

26. Morris RG, Barthelemy M. Transport on coupled spatial networks. Physical Review Letters. 2012; 109(12):128703. https://doi.org/10.1103/PhysRevLett.109.128703 PMID: 23006001

27. Li M, Hu MB, Wang BH. Transportation dynamics on coupled networks with limited bandwidth. Scientific Reports. 2016; 6:39175. https://doi.org/10.1038/srep39175 PMID: 27966624

28. Gallotti R, Barthelemy M. Anatomy and efficiency of urban multimodal mobility. Scientific Reports. 2014; 4:6911. https://doi.org/10.1038/srep06911 PMID: 25371238

29. Aleta A, Meloni S, Moreno Y. A Multilayer perspective for the analysis of urban transportation systems. Scientific Reports. 2017; 7:44359. https://doi.org/10.1038/srep44359 PMID: 28295015

30. Callaway DS, Newman ME, Strogatz SH, Watts DJ. Network robustness and fragility: percolation on random graphs. Physical Review Letters. 2000; 85(25):5468–5471. https://doi.org/10.1103/PhysRevLett.85.5468 PMID: 11136023

31. Parshani R, Buldyrev SV, Havlin S. Interdependent networks: reducing the coupling strength leads to a change from a first to second order percolation transition. Physical Review Letters. 2010; 105(4):048701. https://doi.org/10.1103/PhysRevLett.105.048701 PMID: 20867893

32. Karrer B, Newman MEJ, Zdeborová L. Percolation on sparse networks. Physical Review Letters. 2014; 113(20):208702. https://doi.org/10.1103/PhysRevLett.113.208702 PMID: 25432059

33. Radicchi F. Percolation in real interdependent networks. Nature Physics. 2015; 11(7):597–602. https://doi.org/10.1038/nphys3374

34. Hackett A, Cellai D, Gómez S, Arenas A, Gleeson JP. Bond Percolation on Multiplex Networks. Physical Review X. 2016; 6(2):021002. https://doi.org/10.1103/PhysRevX.6.021002

35. Santoro A, Nicosia V. Optimal percolation in correlated multilayer networks with overlap. Physical Review Research. 2020; 2(3):033122. https://doi.org/10.1103/PhysRevResearch.2.033122

36. Li M, Liu RR, Lü L, Hu MB, Xu S, Zhang YC. Percolation on complex networks: Theory and application. Physics Reports 2021; 907:1–68. https://doi.org/10.1016/j.physrep.2021.02.003

37. Alava M, Moukarzel CF. Transport on percolation clusters with power-law distributed bond strengths. Physical Review E. 2003; 67(5 Pt 2):056106. https://doi.org/10.1103/PhysRevE.67.056106 PMID: 12786219

38. Li D, Fu B, Wang Y, Lu G, Berezin Y, Stanley HE, et al. Percolation transition in dynamical traffic network with evolving critical bottlenecks. Proceedings of the National Academy of Sciences of the U S A. 2015; 112(3):669–672. https://doi.org/10.1073/pnas.1419185112 PMID: 25552558

39. Zeng G, Li D, Guo S, Gao L, Gao Z, Stanley HE, et al. Switch between critical percolation modes in city traffic dynamics. Proceedings of the National Academy of Sciences of the U S A. 2019; 116(1):23–28. https://doi.org/10.1073/pnas.1801545116 PMID: 30591562

40. Hamedmoghadam H, Jalili M, Vu HL, Stone L. Percolation of heterogeneous flows uncovers the bottlenecks of infrastructure networks. Nature Communications. 2021; 12(1):1254. https://doi.org/10.1038/s41467-021-21483-y PMID: 33623037

41. Ambühl L, Menendez M, González MC. Understanding congestion propagation by combining percolation theory with the macroscopic fundamental diagram. Communications Physics. 2023; 6:26. https://doi.org/10.1038/s42005-023-01144-w PMID: 38665407

42. Ford LR, Fulkerson DR. Maximal Flow Through a Network. Canadian Journal of Mathematics Journal Canadien de Mathematiques. 1956; 8:399–404. https://doi.org/10.4153/CJM-1956-045-5

43. Ford LR, Fulkerson DR. Flows in Networks. Princetion: Princeton University Press; 1962.

44. Lee DS, Rieger H. Maximum flow and topological structure of complex networks. EPL. 2005; 73(3):471. https://doi.org/10.1209/epl/i2005-10407-5

45. Dwivedi A, Yu X. A maximum-flow-based complex network approach for power system vulnerability analysis. IEEE transactions on industrial informatics / a publication of the IEEE Industrial Electronics Society. 2013; 9(1):81–88. https://doi.org/10.1109/TII.2011.2173944

46. Cai M, Liu J, Cui Y. Network Robustness Analysis Based on Maximum Flow. Frontiers in Physics. 2021; 9:792410. https://doi.org/10.3389/fphy.2021.792410

47. Pittel B, Spencer J, Wormald N. Sudden Emergence of a Giantk-Core in a Random Graph. Journal of Combinatorial Theory Series B. 1996; 67(1):111–151. https://doi.org/10.1006/jctb.1996.0036

48. Dorogovtsev SN, Goltsev AV, Mendes JFF. k-Core organization of complex networks. Physical Review Letters. 2006; 96(4):040601. https://doi.org/10.1103/PhysRevLett.96.040601 PMID: 16486798

49. Gallagher RJ, Young JG, Welles BF. A clarified typology of core-periphery structure in networks. Science Advances. 2021; 7:eabc9800. https://doi.org/10.1126/sciadv.abc9800 PMID: 33731343

50. Verma T, Araújo NAM, Herrmann HJ. Revealing the structure of the world airline network. Scientific Reports. 2014; 4:5638. https://doi.org/10.1038/srep05638 PMID: 25005934

51. Verma T, Russmann F, Araújo NAM, Nagler J, Herrmann HJ. Emergence of core–peripheries in networks. Nature Communications. 2016; 7:10441. https://doi.org/10.1038/ncomms10441 PMID: 26822856

52. Kostoska O, Mitikj S, Jovanovski P, Kocarev L. Core-periphery structure in sectoral international trade networks: A new approach to an old theory. PLOS ONE. 2020; 15(4):e0229547. https://doi.org/10.1371/journal.pone.0229547 PMID: 32240201

53. Kojaku S, Xu M, Xia H, Masuda N. Multiscale core-periphery structure in a global liner shipping network. Scientific Reports. 2019; 9(1):404. https://doi.org/10.1038/s41598-018-35922-2 PMID: 30674915

54. Dong L, Li R, Zhang J, Di Z. Population-weighted efficiency in transportation networks. Scientific Reports. 2016; 6:26377. https://doi.org/10.1038/srep26377 PMID: 27230706

55. Li R, Gao S, Luo A, Yao Q, Chen B, Shang F, et al. Gravity model in dockless bike-sharing systems within cities. Physical Review E. 2021; 103(1-1):012312. https://doi.org/10.1103/PhysRevE.103.012312 PMID: 33601646

56. Beuthe M, Jourquin B, Geerts JF, Koul à Ndjang' Ha C. Freight transportation demand elasticities: a geographic multimodal transportation network analysis. Transportation Research Part E: Logistics and Transportation Review. 2001; 37(4):253–266. https://doi.org/10.1016/S1366-5545(00)00022-3

57. Mudchanatongsuk S, Ordóñez F, Liu J. Robust solutions for network design under transportation cost and demand uncertainty. The Journal of the Operational Research Society. 2008; 59(5):652–662. https://doi.org/10.1057/palgrave.jors.2602362

58. Kujala R, Weckström C, Darst RK, Mladenović MN, Saramäki J. A collection of public transport network data sets for 25 cities. Scientific Data. 2018; 5:180089. https://doi.org/10.1038/sdata.2018.89 PMID: 29762553

59. Welch TF, Widita A. Big data in public transportation: a review of sources and methods. Transport Reviews. 2019; 39(6):795–818. https://doi.org/10.1080/01441647.2019.1616849

60. Carmi S, Wu Z, Havlin S, Stanley HE. Transport in networks with multiple sources and sinks. EPL. 2008; 84(2):28005. https://doi.org/10.1209/0295-5075/84/28005

61. Hagberg A, Schult D, Swart P, Hagberg JM. Exploring network structure, dynamics, and function using NetworkX; 2008.

62. Barabasi AL, Albert R. Emergence of scaling in random networks. Science. 1999; 286(5439):509–512. https://doi.org/10.1126/science.286.5439.509 PMID: 10521342

63. Rossi R, Ahmed N. The Network Data Repository with Interactive Graph Analytics and Visualization. Proceedings of the AAAI Conference on Artificial Intelligence. 2015;29(1).

64. Borgatti SP, Everett MG. Models of core/periphery structures. Social Networks 2000; 21(4):375–395. https://doi.org/10.1016/S0378-8733(99)00019-2

65. Karrer B, Newman MEJ. Stochastic blockmodels and community structure in networks. Physical Review E. 2011; 83(1 Pt 2):016107. https://doi.org/10.1103/PhysRevE.83.016107 PMID: 21405744